Galilean invariance restoration on the lattice

Ning Li, Serdar Elhatisari, Evgeny Epelbaum, Dean Lee, Bingnan Lu, and Ulf-G. Meißner

Galilean invariance restoration on the lattice

Ning Li,[1] Serdar Elhatisari,[2, 3] Evgeny Epelbaum,[4] Dean Lee,[1, 5] Bingnan Lu,[1] and Ulf-G. Meißner[2, 6, 7]

[1]*Facility for Rare Isotope Beams and Department of Physics and Astronomy, Michigan State University, MI 48824, USA*
[2]*Helmholtz-Institut für Strahlen- und Kernphysik and Bethe Center for Theoretical Physics, Universität Bonn, D-53115 Bonn, Germany*
[3]*Faculty of Engineering, Karamanoglu Mehmetbey University, Karaman 70100, Turkey*
[4]*Ruhr University Bochum, Faculty of Physics and Astronomy,*
Institute for Theoretical Physics II, D-44870 Bochum, Germany
[5]*Department of Physics, North Carolina State University, Raleigh, NC 27695, USA*
[6]*Institute for Advanced Simulation, Institut für Kernphysik,*
and Jülich Center for Hadron Physics, Forschungszentrum Jülich, D-52425 Jülich, Germany
[7]*Tbilisi State University, 0186 Tbilisi, Georgia*

We consider the breaking of Galilean invariance due to different lattice cutoff effects in moving frames and a nonlocal smearing parameter which is used in the construction of the nuclear lattice interaction. The dispersion relation and neutron-proton scattering phase shifts are used to investigate the Galilean invariance breaking effects and ways to restore it. For S-wave channels, $^1S_0$ and $^3S_1$, we present the neutron-proton scattering phase shifts in moving frames calculated using both Lüscher's formula and the spherical wall method, as well as the dispersion relation. For the P and D waves, we present the neutron-proton scattering phase shifts in moving frames calculated using the spherical wall method. We find that the Galilean invariance breaking effects stemming from the lattice artifacts partially cancel those caused by the nonlocal smearing parameter. Due to this cancellation, the Galilean invariance breaking effect is small, and the Galilean invariance can be restored by introducing Galilean invariance restoration operators.

I. INTRODUCTION

Chiral effective field theory (EFT) allows one to construct the nuclear force systematically in powers of Q/Λ_χ, where Q is a soft scale (pion mass, transferred momenta, etc), while Λ_χ (≈ 0.6 GeV) is the pertinent hard scale [1–4]. In chiral EFT, the most important contribution appears at leading order (LO) or order $(Q/\Lambda_\chi)^0$, the second most important contribution at next-to-leading order (NLO) or order $(Q/\Lambda_\chi)^2$, the third most important contribution at next-to-next-to-leading order (N2LO) or order $(Q/\Lambda_\chi)^3$, and so on. According to the power counting of chiral EFT, the LO nucleon-nucleon (NN) interaction includes the static one-pion-exchange potential (OPEP) as well as momentum independent contact interactions, the NLO NN interaction includes the leading two-pion-exchange potential (TPEP) and contact interactions with two derivatives, the N2LO interaction includes only corrections to the TPEP, and the N3LO NN interaction includes further corrections to the OPEP and sub-leading TPEP as well as contact interactions with four derivatives. See [5, 6] for review papers on chiral nuclear EFT.

In the past decades, nuclear lattice effective field theory (NLEFT) combining Monte Carlo simulations on a space-time grid and nuclear forces derived within chiral EFT has become a powerful tool for *ab initio* calculations of the few- and many-body problems. NLEFT has been widely used to study nuclear structure [7–9] and nuclear reactions [10]. See [11] for an early review article. Since NLEFT is powerful for *ab initio* calculations, getting an efficient and precise nuclear force is particularly important, which is a more difficult task than in the continuum due to the lattice artifacts stemming from the nonzero lattice spacing. To reduce the lattice artifacts, non-locally smeared operators were introdued in [12]. With only a few parameters, the binding energies of nuclei with nucleons $A \leq 20$ are produced with good precision. In Ref. [13] , these non-locally smeared operators were extended up to next-to-next-to-next-to-leading order (N3LO) in chiral EFT for neutron-proton scattering.

However, in a lattice-regularized system, finite-lattice spacing effects are different in moving frames. This breaks the Galilean invariance [14], which is the statement that the laws of Newtonian physics for a non-relativistic system are independent of the velocity of the center of mass. There is also some breaking of Galilean invariance caused by the nonlocal smearing parameter s_{NL} we use in the construction of the lattice interaction as it induces the explicit dependence of the lattice interaction on the momentum of the center of mass. In the present work, we focus on the lattice calculations with lattice spacing $a = 1.32$ fm and the N3LO nucleon-nucleon interactions from [13]. We quantify the effects of Galilean invariance breaking by analyzing the dispersion relation and neutron-proton scattering phase shifts in moving frames. We also show how to restore the Galilean invariance by including the contribution of the Galilean invariance restoration operators. This is the main finding of this paper that will be used in future NLEFT investigations.

The paper is organized as follows. After the introduction, in section II we will present the formalism including the lattice nucleon-nucleon interaction up to N3LO in chiral EFT, the Lüscher's formula and spherical wall method used to extract the scattering phase shifts. Then, we present the numerical results and make discussions in section III. Finally, we summarize our results in section IV.

II. FORMALISM

Before present the details of our formalism, it is useful to state some conventions appearing many times in the present paper. Throughout this work we use a for the spatial lattice spacing, L denotes the number of lattice points in each spacial direction, and $\mathbf{P}$ is the momentum of the center of mass. All parameters and operators are first expressed in lattice units, which correspond to the physical values multiplied by appropriate powers of a. Our final results are presented in physical units.

Different from our previous calculations, where the transfer matrix formalism was used, here we utilize the Hamiltonian formalism since the transfer matrix formalism can induce additional breaking of Galilean invariance due to the nonzero temporal lattice spacing. In our calculation, the Hamiltonian has the form,

$$H = H_{\mathrm{free}} + V_{2\mathrm{N}}^{\mathrm{short}} + V_{2\mathrm{N}}^{\mathrm{long}}. \tag{1}$$

For the free Hamiltonian we use an $O(a^4)$-improved action of the form [11],

$$H_{\mathrm{free}} = \frac{49}{12m_N} \sum_{\mathbf{n}} a^\dagger(\mathbf{n})a(\mathbf{n}) - \frac{3}{4m_N} \sum_{\mathbf{n},i} \sum_{\langle \mathbf{n'} \mathbf{n} \rangle_i} a^\dagger(\mathbf{n'})a(\mathbf{n})$$

$$+ \frac{3}{40m_N} \sum_{\mathbf{n},i} \sum_{\langle\langle \mathbf{n'} \mathbf{n} \rangle\rangle_i} a^\dagger(\mathbf{n'})a(\mathbf{n}) - \frac{1}{180m_N} \sum_{\mathbf{n},i} \sum_{\langle\langle\langle \mathbf{n'} \mathbf{n} \rangle\rangle\rangle_i} a^\dagger(\mathbf{n'})a(\mathbf{n}), \tag{2}$$

where $a^\dagger$ and a are the creation and annihilation operators for a nucleon, respectively, and m_N denotes the nucleon mass. The number of brackets under the sum refer to the nearest, next-to-nearest and next-to-next-to-nearest neighbors used in the representation of the derivatives. $V_{2\mathrm{N}}^{\mathrm{short}}$ is the short-range nucleon-nucleon interaction accounted by contact interactions while $V_{2\mathrm{N}}^{\mathrm{long}}$ denotes the long-range NN interaction provided by the pion-exchange potentials.

A. Nucleon-nucleon interaction on the lattice

Up to N3LO in chiral EFT, the short-range nucleon-nucleon interaction includes contact interactions at LO, NLO and N3LO,

$$V_{2N}^{short} = V_{contact}^{(Q/\Lambda_\chi)^0} + V_{contact}^{(Q/\Lambda_\chi)^2} + V_{contact}^{(Q/\Lambda_\chi)^4}. \tag{3}$$

At LO, two non-locally smeared contact operators were introduced in Ref. [13]. These read

$$V_{{}^1S_0,(Q/\Lambda_\chi)^0} = \sum_{I_z=-1,0,1} \left[O_{0,0,0,0,1,I_z}^{0,s_{NL}}(\mathbf{n}) \right]^\dagger O_{0,0,0,0,1,I_z}^{0,s_{NL}}(\mathbf{n}), \tag{4}$$

for the ${}^1S_0$ channel, and

$$V_{{}^3S_1,(Q/\Lambda_\chi)^0} = \sum_{J_z=-1,0,1} \left[O_{1,0,1,J_z,0,0}^{0,s_{NL}}(\mathbf{n}) \right]^\dagger O_{1,0,1,J_z,0,0}^{0,s_{NL}}(\mathbf{n}), \tag{5}$$

for the ${}^3S_1$ channel. We refer to App. A for the definitions of the pair creation operator $O^\dagger$ and pair annihilation operator O. The contact operators at NLO and N3LO can be written in a similar manner. Their specific expressions which are not given here for simplicity can be found in [13].

Additionally, we also include an SU(4)-invariant short-range operator at LO, which has been shown to be important for nuclear binding [12, 15],

$$V_0 = \frac{C_0}{2} : \sum_{\mathbf{n'},\mathbf{n},\mathbf{n''}} \sum_{i',j'} a_{i',j'}^{s_{NL}\dagger}(\mathbf{n'}) a_{i',j'}^{s_{NL}}(\mathbf{n'}) f_{s_L}(\mathbf{n'}-\mathbf{n}) f_{s_L}(\mathbf{n}-\mathbf{n''}) \sum_{i'',j''} a_{i'',j''}^{s_{NL}\dagger}(\mathbf{n''}) a_{i'',j''}^{s_{NL}}(\mathbf{n''}) :, \tag{6}$$

where :: denotes normal ordering, and the local smearing function $f_{s_L}(\mathbf{n})$ is defined as

$$f_{s_L} = \begin{cases} 1, & |\mathbf{n}| = 0, \\ s_L, & |\mathbf{n}| = 1, \\ 0, & \text{otherwise.} \end{cases} \tag{7}$$

The index i corresponds to nucleon spin, and the index j corresponds to nucleon isospin. The dressed creation operator $a^{s_{NL}\dagger}$ and annihilation operator $a^{s_{NL}}$ are defined respectively as

$$a_{i,j}^{s_{NL}\dagger}(\mathbf{n}) = a_{i,j}^\dagger(\mathbf{n}) + s_{NL} \sum_{|\mathbf{n'}|=1} a_{i,j}^\dagger(\mathbf{n}+\mathbf{n'}). \tag{8}$$

and

$$a_{i,j}^{s_{NL}}(\mathbf{n}) = a_{i,j}(\mathbf{n}) + s_{NL} \sum_{|\mathbf{n'}|=1} a_{i,j}(\mathbf{n}+\mathbf{n'}), \tag{9}$$

We use the dressed creation (annihilation) operator to create (annihilate) the nucleon placed at the exact lattice site as well as the nucleon located at its nearest-neighbor lattice sites. In this manner, some of the lattice artifacts induced by the nonzero lattice spacing can be removed. However, the nonzero value of s_{NL} leads to a breaking of Galilean invariance because it makes the NN interaction depend on the velocity of the center of mass.

For the long-range interaction, we include the OPEP at LO, and the two-pion-exchange potentials at NLO, N2LO, and N3LO.

$$V_{2N}^{long} = V_{OPE}^{(Q/\Lambda_\chi)^0} + V_{TPE}^{(Q/\Lambda_\chi)^2} + V_{TPE}^{(Q/\Lambda_\chi)^3} + V_{TPE}^{(Q/\Lambda_\chi)^4}. \tag{10}$$

The one-pion exchange potential V_{OPE} has the form

$$V_{OPE} = -\frac{g_A^2}{8F_\pi^2} \sum_{\mathbf{n'},\mathbf{n},S',S,I} : \rho_{S',I}(\mathbf{n'}) f_{S'S}(\mathbf{n'}-\mathbf{n}) \rho_{S,I}(\mathbf{n}) :, \tag{11}$$

where $f_{S'S}$ is defined as

$$f_{S'S}(\mathbf{n'}-\mathbf{n}) = \frac{1}{L^3} \sum_{\mathbf{q}} \frac{Q(q_{S'}) Q(q_S) \exp[-i\mathbf{q}\cdot(\mathbf{n'}-\mathbf{n}) - b_\pi(\mathbf{q}^2 + M_\pi^2)]}{\mathbf{q}^2 + M_\pi^2}, \tag{12}$$

and each lattice momentum component q_S is an integer multiplied by $2\pi/L$. The function $Q(q_S)$ is given by

$$Q(q_S) = \frac{3}{2}\sin(q_S) - \frac{3}{10}\sin(2q_S) + \frac{1}{30}\sin(3q_S), \tag{13}$$

which equals q_S up to correction of order q_S^7. We use the definition of Eq. (13) for the nucleon momentum on the lattice to remove the finite lattice volume effects. We include the parameter b_π to regularize the short-range behavior of the OPEP. As in previous calculations, we set $b_\pi = 0.25$ in lattice units. For calculations with lattice spacing $a = 1.32$ fm, this is equivalent to $\Lambda = 300$ MeV in the form factor

$$F(\mathbf{q}) = \exp\left[-\frac{(\mathbf{q}^2 + m_\pi^2)}{\Lambda^2}\right]. \tag{14}$$

We use the combination $\mathbf{q}^2 + M_\pi^2$ in the exponential as suggested in [16] as a momentum-space regulator which does not affect the long-distance behavior of the pion-exchange potential.

As we are solving non-relativistic Schrödinger equations, we neglect the relativistic corrections to the NN force at N3LO stemming from the $1/m_N^2$-corrections to the static OPEP and $1/m_N$-corrections to static TPEP including spin-orbital interacting terms [16, 17]. As a result, the long-range pion-exchange potential is totally local and independent of the velocity of the center of mass. Therefore, this part does not break Galilean invariance. Instead of providing the lengthy expressions of two-pion-exchange potential, we refer the reader to [16–19] for the specific expressions.

B. Galilean invariance restoration operators

To restore the Galilean invariance for the two-nucleon system, we introduce the pair hopping terms. We first illustrate with pointlike operators corresponding to the product of total nucleon densities,

$$V_{\mathrm{GIR}} = V_{\mathrm{GIR}}^0 + V_{\mathrm{GIR}}^1 + V_{\mathrm{GIR}}^2, \tag{15}$$

where

$$V_{\mathrm{GIR}}^0 = C_{\mathrm{GIR}}^0 \sum_{\mathbf{n},i,j,i',j'} a_{i,j}^\dagger(\mathbf{n})a_{i',j'}^\dagger(\mathbf{n})a_{i',j'}(\mathbf{n})a_{i,j}(\mathbf{n}) \tag{16}$$

denotes no hopping,

$$V_{\mathrm{GIR}}^1 = C_{\mathrm{GIR}}^1 \sum_{\mathbf{n},i,j,i',j'} \sum_{|\mathbf{n}'|=1} a_{i,j}^\dagger(\mathbf{n}+\mathbf{n}')a_{i',j'}^\dagger(\mathbf{n}+\mathbf{n}')a_{i',j'}(\mathbf{n})a_{i,j}(\mathbf{n}) \tag{17}$$

is the nearest-neighbor hopping term, and

$$V_{\mathrm{GIR}}^2 = C_{\mathrm{GIR}}^2 \sum_{\mathbf{n},i,j,i',j'} \sum_{|\mathbf{n}'|=\sqrt{2}} a_{i,j}^\dagger(\mathbf{n}+\mathbf{n}')a_{i',j'}^\dagger(\mathbf{n}+\mathbf{n}')a_{i',j'}(\mathbf{n})a_{i,j}(\mathbf{n}) \tag{18}$$

is the next-to-nearest-neighbor hopping term for the nucleon-nucleon pair.

Let us write $|\mathbf{P}\rangle$ as a two-body bound-state wave function with total momentum $\mathbf{P}$. We note that $\langle\mathbf{P}|V_{\mathrm{GIR}}^0|\mathbf{P}\rangle$ is independent of $\mathbf{P}$, and so we have

$$\langle\mathbf{P}|V_{\mathrm{GIR}}^0|\mathbf{P}\rangle = C_{\mathrm{GIR}}^0\langle\mathbf{0}|V_{\mathrm{GIR}}^0|\mathbf{0}\rangle, \tag{19}$$

where $|\mathbf{0}\rangle$ is the two-body bound-state wave function with zero total momentum. Furthermore,

$$\langle\mathbf{P}|V_{\mathrm{GIR}}^1|\mathbf{P}\rangle = 2C_{\mathrm{GIR}}^1\left[\cos(P_x) + \cos(P_y) + \cos(P_z)\right]\langle\mathbf{0}|V_{\mathrm{GIR}}^0|\mathbf{0}\rangle, \tag{20}$$

and

$$\langle\mathbf{P}|V_{\mathrm{GIR}}^2|\mathbf{P}\rangle = 4\left[\cos(P_x)\cos(P_y) + \cos(P_y)\cos(P_z) + \cos(P_z)\cos(P_x)\right]\langle\mathbf{0}|V_{\mathrm{GIR}}^0|\mathbf{0}\rangle. \tag{21}$$

Combining the hopping term with the contact terms we can construct the GIR operators. For simplicity, we only take the lowest-order contact operator of each channel to construct the GIR operators. For example, the GIR operator for the $^1S_0$ channel

reads

$$V_{\text{GIR}}^{^1S_0} = C_{\text{GIR},0}^{^1S_0} \sum_{\mathbf{n}} \sum_{I_z=-1,0,1} \left[O_{0,0,0,0,1,I_z}^{0,s_{NL}}(\mathbf{n}) \right]^\dagger O_{0,0,0,0,1,I_z}^{0,s_{NL}}(\mathbf{n})$$

$$+ C_{\text{GIR},1}^{^1S_0} \sum_{\mathbf{n}} \sum_{|\mathbf{n}'|=1} \sum_{I_z=-1,0,1} \left[O_{0,0,0,0,1,I_z}^{0,s_{NL}}(\mathbf{n}+\mathbf{n}') \right]^\dagger O_{0,0,0,0,1,I_z}^{0,s_{NL}}(\mathbf{n})$$

$$+ C_{\text{GIR},2}^{^1S_0} \sum_{\mathbf{n}} \sum_{|\mathbf{n}'|=\sqrt{2}} \sum_{I_z=-1,0,1} \left[O_{0,0,0,0,1,I_z}^{0,s_{NL}}(\mathbf{n}+\mathbf{n}') \right]^\dagger O_{0,0,0,0,1,I_z}^{0,s_{NL}}(\mathbf{n}), \tag{22}$$

whereas that for the $^1P_1$ channel is

$$V_{\text{GIR}}^{^1P_1} = C_{\text{GIR},0}^{^1P_1} \sum_{\mathbf{n}} \sum_{J_z=-1,0,1} \left[O_{0,1,1,J_z,0,0}^{0,s_{NL}}(\mathbf{n}) \right]^\dagger O_{0,1,1,J_z,0,0}^{0,s_{NL}}(\mathbf{n})$$

$$+ C_{\text{GIR},1}^{^1P_1} \sum_{\mathbf{n}} \sum_{|\mathbf{n}'|=1} \sum_{J_z=-1,0,1} \left[O_{0,1,1,J_z,0,0}^{0,s_{NL}}(\mathbf{n}+\mathbf{n}') \right]^\dagger O_{0,1,1,J_z,0,0}^{0,s_{NL}}(\mathbf{n})$$

$$+ C_{\text{GIR},2}^{^1P_1} \sum_{\mathbf{n}} \sum_{|\mathbf{n}'|=\sqrt{2}} \sum_{J_z=-1,0,1} \left[O_{0,1,1,J_z,0,0}^{0,s_{NL}}(\mathbf{n}+\mathbf{n}') \right]^\dagger O_{0,1,1,J_z,0,0}^{0,s_{NL}}(\mathbf{n}). \tag{23}$$

Using these GIR operators, we can restore Galilean invariance for each channel by finely tuning $C_{\text{GIR},i}(i = 0, 1, 2)$ with the constraint,

$$C_{\text{GIR},0} + 6C_{\text{GIR},1} + 12C_{\text{GIR},2} = 0, \tag{24}$$

which is the requirement that the GIR correction should be vanishing for zero total momentum. Specifically, we take the Nijmegen phase shifts as input to determine the LECs for each channel in the rest frame, and then determine the coefficients $C_{\text{GIR},i}$ by fitting the phase shifts in the boosted frames, where the lattice results in the rest frame are taken as input. For example, two LECs for $^1P_1$ are fixed at N3LO without GIR, then two additional coefficients, $C_{\text{GIR},i}$, are used to restore the Galilean invariance.

C. Lüscher's formula

In [20], Lüscher derived a simple formula connecting the two-body S-wave scattering phase shift δ_0 with the energy levels calculated in the lattice framework. It reads

$$\exp\left(2i\delta_0(k)\right) = \frac{\zeta_{00}(1; q^2) + i\pi^{3/2}q}{\zeta_{00}(1; q^2) - i\pi^{3/2}q}, \tag{25}$$

where

$$q = \frac{kL}{2\pi}, \tag{26}$$

and

$$\zeta_{00}(s; q^2) = \frac{1}{\sqrt{4\pi}} \sum_{\mathbf{n} \in Z^3} (\mathbf{n}^2 - q^2)^{-s} \tag{27}$$

is the zeta function which is convergent when $\text{Re}(s) > 3/2$, and can be analytically continued to $s = 1$. Then, this formula was generalized to moving frames with center-of-mass momentum $\mathbf{P} = (2\pi/L)\mathbf{k}$ [21–24],

$$\delta_0(k) = \arctan\left(\frac{\gamma q\pi^{3/2}}{\zeta_{00}^{\mathbf{d}}(1; q^2)}\right), \tag{28}$$

where

$$\zeta_{00}^{\mathbf{d}}(s; q^2) = \frac{1}{\sqrt{4\pi}} \sum_{\mathbf{r} \in P_d} (\mathbf{r}^2 - q^2)^{-s}, \tag{29}$$

is the generalized zeta function. The summation region $P_{\mathbf{d}}$ is defined as

$$P_{\mathbf{d}} = \left\{ \mathbf{r} \in R^3 | \mathbf{r} = \gamma^{-1}(\mathbf{n} + \mathbf{d}/2), \mathbf{n} \in Z^3 \right\}, \tag{30}$$

where γ is the Lorentz factor and $\gamma^{-1}\mathbf{n}$ is the shorthand notation for $\gamma^{-1}\mathbf{n}_\| + \mathbf{n}_\perp$. It is easy to check that formulae Eq. (25) and (28) are the same when $\mathbf{P} = 0$. The expressions for the numerical calculation of the generalized zeta function can be found in Refs. [21, 25]. Refer to [25–28] for several interesting lattice QCD calculations in the moving frames.

In our calculation, the Lüscher formula is applied to calculate the neutron-proton scattering phase shifts for only the S-wave channels. This is done because Lüscher's formula is not an efficient method to extract the scattering phase shifts for the P, D and higher partial waves. Even for $^3S_1$, we find a small discrepancy between the results using Lüscher's formula and those using the spherical wall method. This is because there is a systematic error in the mixing of different channels when using the Lüscher's formula. We will come back to this later.

D. Spherical wall method

In addition to Lüscher's formula, the spherical wall method is another approach to extract the scattering phase shifts. Differently from Lüscher's formula connecting the scattering phase shifts with the energy levels, the spherical wall method extracts the scattering phase shifts from the wave function. To calculate the scattering phase shifts and mixing angles using the spherical wall method, we first construct radial wave functions in a moving frame with momentum $\mathbf{P}$ through the spherical harmonics with quantum numbers (l, l_z) [29, 30],

$$|r\rangle_{\mathbf{P}}^{l,l_z} = \sum_{\hat{\mathbf{r}}'} \exp(-i\mathbf{P} \cdot \mathbf{r}')Y_{l,l_z}(\hat{\mathbf{r}}')\delta_{|\mathbf{r}'|=r}|\mathbf{r}'\rangle, \tag{31}$$

where $\hat{r}'$ runs over all lattice sites having the same radial lattice distance, and $\mathbf{P} = (2\pi/L)\mathbf{k}$ is the quantized center-of-mass momentum on the lattice. Using this definition for the radial wave function, the Hamiltonian matrix over a three-dimensional lattice can be reduced to a one-dimensional radial Hamiltonian, $H_{\mathbf{r},\mathbf{r}'} \rightarrow H_{r,r'}$.

After solving the Schödinger equation, the phase shifts and mixing angles can be extracted from the radial wave function in the region where the NN force is vanishing. In this range, the wave function is a superposition of the incoming plane wave and outgoing radial wave which can be expanded as [13, 29]

$$\langle r|k,l\rangle = A_j h_l^{(1)}(kr) + B_j h_l^{(2)}(kr), \tag{32}$$

where $h_l^{(1)}(kr)$ and $h_l^{(2)}(kr)$ are the spherical Hankel functions. $k = \sqrt{2\mu E}$ with μ the reduced mass and E the relative energy of the two-nucleon system. The scattering coefficients A_j and B_j satisfy the relations,

$$B_j = S_j A_j, \tag{33}$$

where $S_j = \exp(2i\delta_j)$ is the S-matrix and δ_j is the phase shift. The phase shift is determined by setting

$$\delta_j = \frac{1}{2i} \log\left(\frac{B_j}{A_j}\right). \tag{34}$$

In the case of the coupled channels with $j > 0$, both of the coupled partial waves, $l = j - 1$ and $l = j + 1$, satisfy Eq. (33), and the S-matrix couples the two channels together. Throughout this work we adopt the so-called Stapp parameterization of the phase shifts and mixing angles for the coupled channels [31],

$$S = \begin{bmatrix} \cos(2\epsilon)\exp\left(2i\delta_{j-1}^{1j}\right) & i\sin(2\epsilon)\exp\left(i\delta_{j-1}^{1j} + i\delta_{j+1}^{1j}\right) \\ i\sin 2\epsilon \exp\left(i\delta_{j-1}^{1j} + i\delta_{j+1}^{1j}\right) & \cos(2\epsilon)\exp\left(2i\delta_{j+1}^{1j}\right) \end{bmatrix}. \tag{35}$$

III. NUMERICAL RESULTS AND DISCUSSION

In our calculation, we first determine the low-energy constants by matching the calculated neutron-proton scattering phase shifts to those from the Nijmegen partial analysis. Then, we boost the two-nucleon system to a moving frame with momenta $\mathbf{P} = (2\pi/L)\mathbf{k}$ and calculate the phase shifts again. From the difference between these two results, we can read off the amount of the Galilean invariance breaking (GIB). We finally restore the Galilean invariance by tuning the coefficient $C_{\text{GIR},i}$ to make the results independent of $\mathbf{P}$. Since the dispersion relation is another good physical quantity to test the GIB, we also calculate it for both S-wave channels, $^1S_0$ and $^3S_1$.
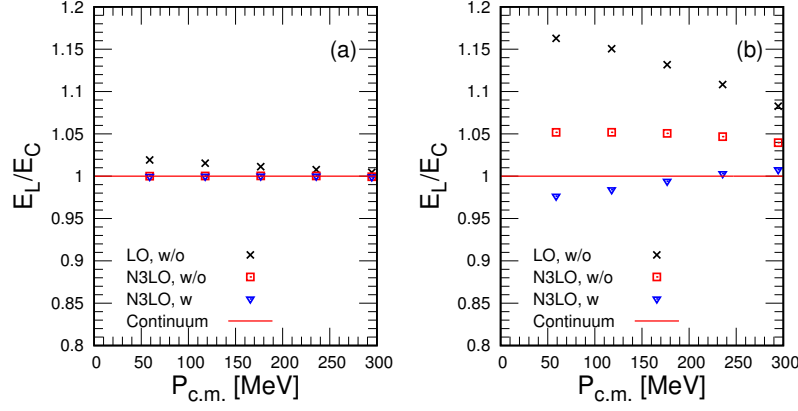
FIG. 1. (Color online) The ratios of the lattice and continuum energy as a function of the momentum of the center of mass. Left panel: $^1S_0$, right panel: $^3S_1$. "w/" means with GIR whereas "w/o" means without GIR.

For lattice parameters, we use the same values as those in one of our previous calculations in Ref. [13], namely, the spatial lattice spacing $a = 1.32$ fm, coefficient for the SU(4) contact potential $C_0 = -0.04455$ l.u. (lattice units), local smearing parameter $s_L = 0.16985$ l.u., and nonlocal smearing parameter $s_{\rm NL} = 0.18566$ l.u.. We use $m_p = 938.272$ MeV and $m_n = 939.565$ MeV for the proton and the neutron mass, respectively. For the charged pion mass, we take $M_{\pi^\pm} = 139.57$ MeV while for the neutral pion mass, we take $M_{\pi^0} = 134.97$ MeV. For the averaged pion mass we use $M_\pi = 138.03$ MeV. Additionally, we use $F_\pi = 92.1$ MeV for the pion decay and $g_A = 1.287$ from the Goldberger-Treiman relation using the pion-nucleon coupling constant from Ref. [32] for the nucleon axial coupling constant, respectively, and $c_1 = -1.10(3)$ GeV^{-1}, $c_2 = 3.57(4)$ GeV^{-1}, $c_3 = -5.54(6)$ GeV^{-1}, and $c_4 = 4.17(4)$ GeV^{-1} [33], for the low-energy constants appearing in the TPEP. For the pion-nucleon LECs d_i entering the chiral N3LO two-pion-exchange poential, we adopt $\bar{d}_1 + \bar{d}_2 = 1.04$ GeV^{-2}, $\bar{d}_3 = -0.48$ GeV^{-2}, $\bar{d}_5 = 0.14$ GeV^{-2} and $\bar{d}_{14} - \bar{d}_{15} = -1.90$ GeV^{-2} [16].

A. Dispersion relation for the S waves

We calculate the dispersion relation for the two S-wave channels, $^1S_0$ and $^3S_1$, of the proton-neutron system in a cubic box of volume $V = (32a)^3$ with lattice spacing $a = 1.32$ fm. To make the effects better visible, we plot the ratios of the lattice and continuum energy as a function of the center-of-mass momentum. The results are shown in Fig. 1. E_L/E_C is the ratio of the lattice and continuum energy. The left plot is for $^1S_0$ while the right plot gives $^3S_1$. We present the results without GIR at both LO and N3LO, which are used to read off the amount of Galilean invariance breaking. We also provide the results including GIR corrections at N3LO.

From the plots, the lattice results for $^1S_0$ are closer to the continuum results that those for $^3S_1$. This is because the state we are boosting in the $^1S_0$ channel is a continuum state rather than bound state. The almost perfect dispersion suggests that it is not an efficient tool to investigating the GIB effect for $^1S_0$. Later, we will apply the proton-neutron scattering phase to study GIB in the $^1S_0$ channel. Differently from the $^1S_0$ case, the dispersion relation is very useful to detect GIB in the $^3S_1$ channel as the ground state in this case is a bound state. From the plots, it is clear that compared to the LO result, the N3LO values are closer to the continuum result. This indicates that there is less GIB effect for the N3LO interaction than for the LO interaction. Further, this indicates that GIB effect stems from the nonlocal smearing parameter partially cancel those caused by the lattice artifacts since there are some non-locally smeared contact terms at NLO and N3LO.

B. S-wave neutron-proton scattering phase shifts

We first calculate the neutron-proton scattering phase shifts for the S-wave channels, $^1S_0$ and $^3S_1$, using Lüscher's formula. In order to obtain results for a wide energy range, we use several cubic boxes with volumes $V = (14a)^3$, $(16a)^3$, and $(18a)^3$. To study the finite volume effects, larger cubic boxes with volume of $V = (24a)^3$, $(26a)^3$ and $(28a)^3$ are also used for the same calculations. We first perform the calculation in the rest-frame, and then boost the proton-neutron system to moving frames with momenta $\mathbf{P} = (2\pi/L)\mathbf{k}$. The results for $^1S_0$ and $^3S_1$ are shown in Figs. 2 and 3, respectively. The plots in top row are the LO results while those in the bottom row are the N3LO results. The left two columns are the results using the smaller boxes whereas the right two columns are the results using the larger boxes. 'w/o' means without GIR corrections whereas 'w/' denotes
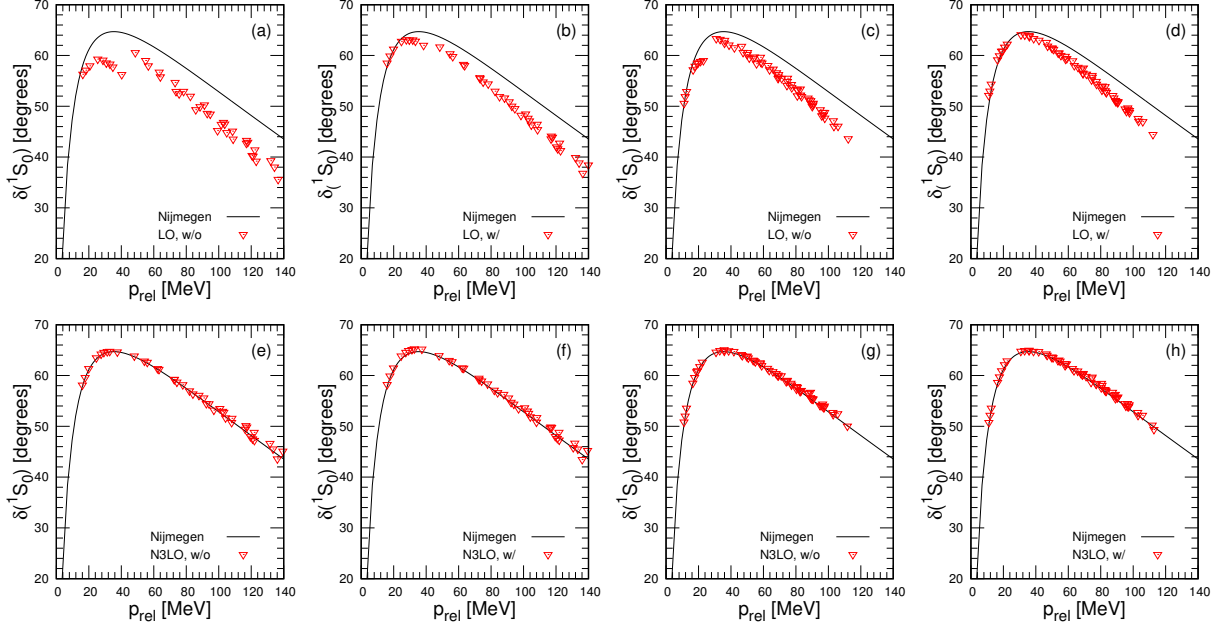
FIG. 2. (Color online) Neutron-proton scattering phase shifts of $^1S_0$ as a function of the relative momenta between the proton and neutron. The Lüscher formula is used to extract the scattering phase shifts. Top row: LO results, bottom row: N3LO results. 'w/o' means without GIR corrections while 'w/' denotes the results after restoring the Galilean invariance. To study the finite volume effects, we did calculations using different size boxes, $L = 14a, 16a, 18a$ for the left two columns and $L = 24a, 26a, 28a$ for the right two columns. In the generalization of the Lüscher's formula to the non-rest frames, the symmetry of the subgroup of the cubic group is applied. However, this symmetry is broken due to the breaking of the Galilean invariance. This leads to the rapid change of the phase shifts at chiral LO. We can see that this behavior goes away after the Galilean invariance is restored.

the results after restoring the Galilean invariance.

From the plots in the top row of Fig. 2, one can see that there is clear GIB at LO although the calculation shows very good dispersion relation. The GIB of $^1S_0$ at LO appears at low momenta, that is for relative momenta between 20 and 40 MeV. The Galilean invariance is restored after including the GIR corrections. It is necessary to mention that the deviation of the lattice results from those of the Nijmegen partial wave analysis is just because these are the LO results. At N3LO, it shows negligible GIB for $^1S_0$, which is consistent with what the dispersion relation indicates. The case for $^3S_1$ is different since the ground state of $^3S_1$ is a bound state. Both the LO and N3LO results show very small GIB. Combining the results of $^1S_0$ and $^3S_1$, we find that the N3LO interaction has less GIB than the LO interaction. This is because the GIB from the non-locally smeared contact interactions at NLO and N3LO accidentally cancel some GIB effects caused by the lattice artifacts due to the nonzero lattice spacing.

We also calculate the scattering phase shifts for $^1S_0$ and $^3S_1$ using the spherical wall method. The spherical wall method works with a one-dimension radial Hamiltonian matrix instead of a full three-dimension matrix. Thus the calculation is much faster than using Lüscher's formula. Meanwhile, in order to reach the region where the NN interaction is vanishing a much larger box should be used. In our calculation, we set $L = 40$ corresponding to radial distance to be $La/2 = 26.4$ fm for $a = 1.32$ fm. To obtain a clear signal of GIB, we boost the proton-neutron system to moving frame with momentum $\mathbf{P} = (2\pi/L)\mathbf{k}$ with $\mathbf{k} = [3,3,3]^T$. The N3LO results are shown in Fig. 4. The small difference of the phase shifts in the two frames with $\mathbf{k} = [0,0,0]^T$ and $\mathbf{k} = [3,3,3]^T$ indicates the Galilean invariance breaking of the interaction is small. Additionally, one also observes small difference of the phase shifts for $^3S_1$ calculated using the spherical wall method from those calculated using the Lüscher's formula. This is because there is a systematic error arising from the unphysical coupling of the $l = 0$ state with $l = 4, 6$, and even higher partial waves using the generalized Lüscher's formula in frames with $\mathbf{P} \neq \mathbf{0}$ [22, 26, 34].

C. Mixing angles, ϵ_1 and ϵ_2, and neutron-proton scattering phase shifts for P and D waves

As the Lüscher formula works well for the S waves but not as accurately for the P, D and even higher partial waves, we continue to calculate the mixing angles, $\epsilon_1(^3S_1 - {^3D_1})$ and $\epsilon_2(^3P_2 - {^3F_2})$, and proton-neutron scattering phase shifts for P and D waves using the spherical wall method. The results are shown in Figs. 5, 6, and 7, respectively.

From the plots, the Galilean invariance breaking for ϵ_1 starts around $p_{\text{rel}} = 120$ MeV while that for ϵ_2 starts around $p_{\text{rel}} =$
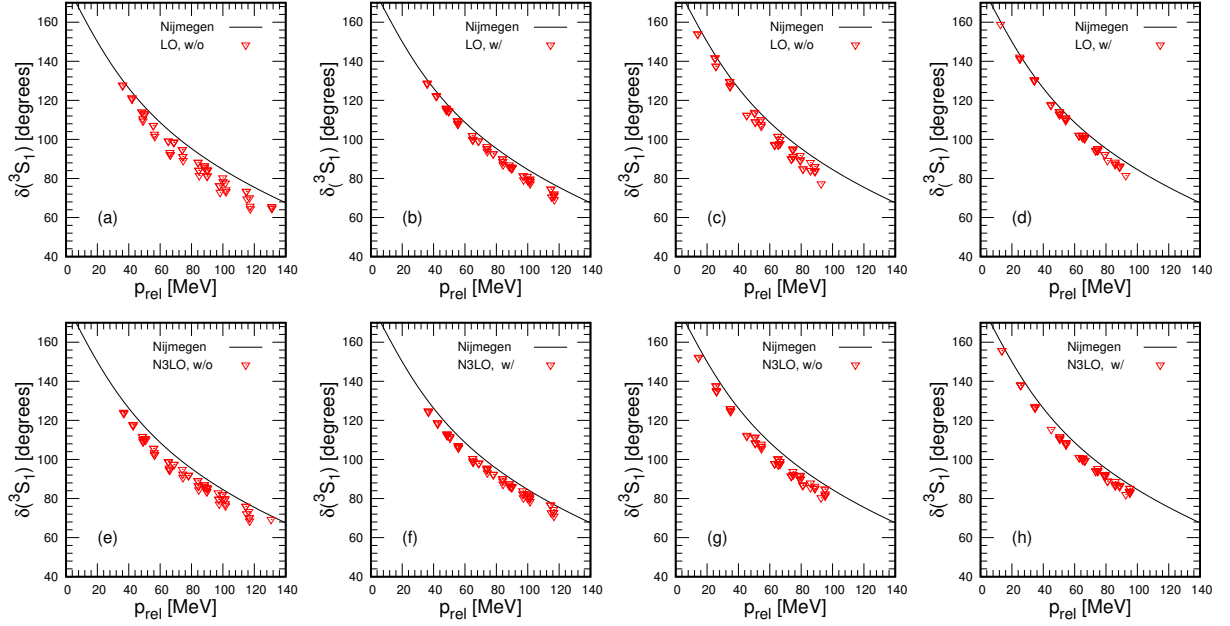
FIG. 3. (Color online) Neutron-proton scattering phase shifts of $^3S_1$ as a function of the relative momenta between the proton and neutron. The Lüscher formula is used to extract the scattering phase shifts. 'w/o' means without GIR corrections while 'w/' denotes the results after restoring the Galilean invariance. To study the finite volume effects, we did calculations using different size boxes, $L = 14a, 16a, 18a$ for the left two columns and $L = 24a, 26a, 28a$ for the right two columns. Top row: LO results, bottom row: N3LO results.
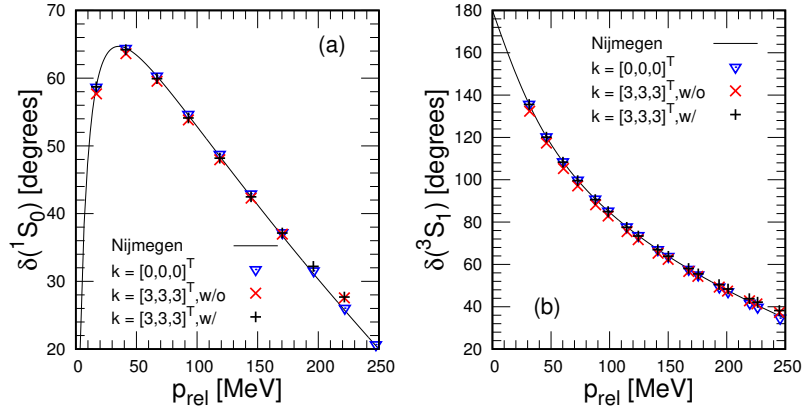
FIG. 4. (Color online) S-wave neutron-proton scattering phase shifts calculated using the spherical wall method as a function of the relative momenta between the two nucleons.

150 MeV. For ϵ_1, after including the GIR correction the Galilean invariance is restored for the whole range $p_{\rm rel} \leq 250$ MeV. For ϵ_2, the GIR correction reduces the GIB very much although not completely.

The behavior of the phase shifts for all four P-wave channels is very similar. The GIB appears in the high-momenta region, and starts around $p_{\rm rel} = 120$ MeV. After including the GIR correction, the GIB is largely removed. Very similarly, GIB also appears in high-momentum region for the D waves. It starts around $p_{\rm rel} = 100$ MeV for $^1D_2$ and $^3D_3$, and around $p_{\rm rel} = 150$ MeV for $^3D_1$ and $^3D_2$. The GIR correction increases the starting points of GIB to around $p_{\rm rel} = 200$ MeV.

IV. CONCLUSIONS

With the rapid development of the high performance computers, nuclear lattice effective field theory has become a powerful tool in *ab initio* calculations of few- and many-body systems. However, getting efficient and precise nuclear forces on the lattice is more difficult than in the continuum due to the lattice artifacts caused by the nonzero lattice spacing. In order to reduce the
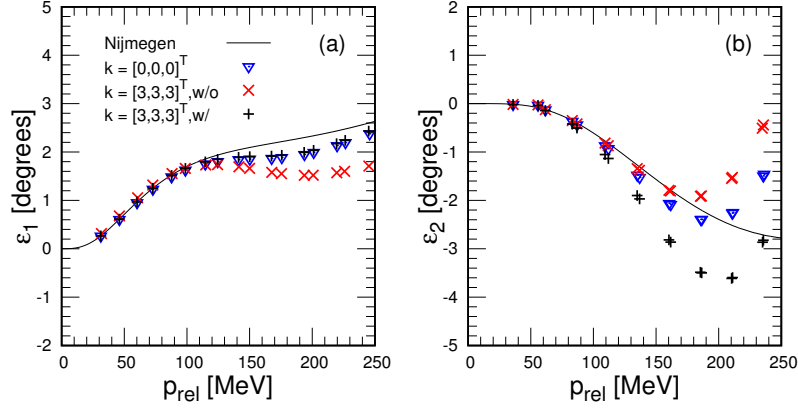
FIG. 5. (Color online) Mixing angles, $\epsilon_1(^3S_1 - {}^3D_1)$ and $\epsilon_2(^3P_2 - {}^3F_2)$, as a function of relative momenta between the proton and neutron. The spherical wall method is used.
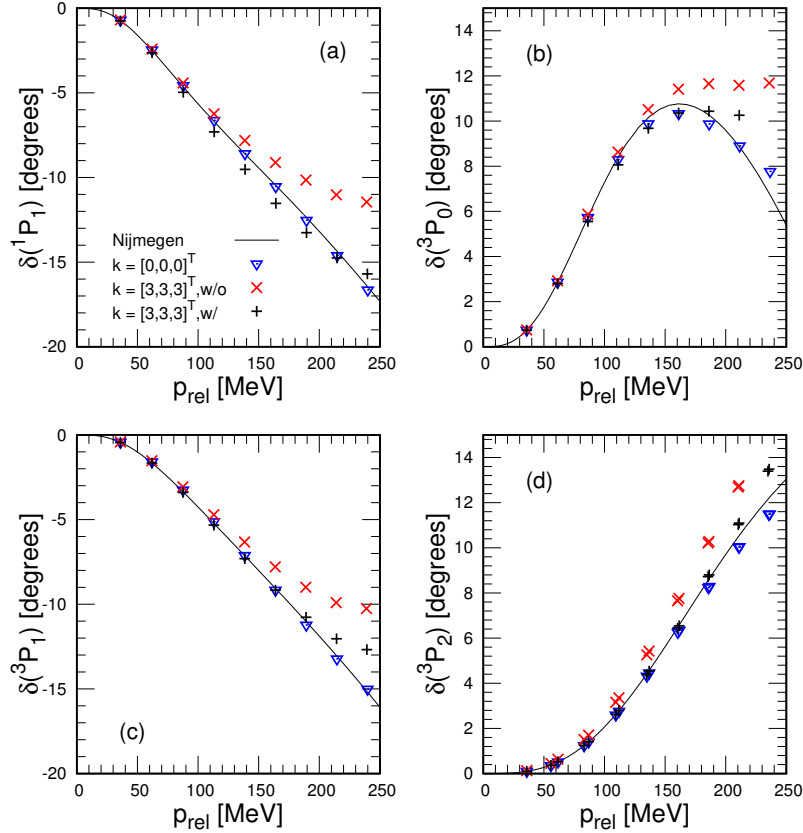

FIG. 6. (Color online) P-wave neutron-proton scattering phase shifts as a function of relative momenta between the proton and neutron. The spherical wall method is used.

lattice artifacts, in [12] non-locally smeared contact operators were introduced. With only a few parameters, the binding energy of nuclei with nucleons up to twenty can be produced with good precision. However, the Galilean invariance is broken due to the nonlocal smearing parameter s_{NL} used to construct the contact operators. Another source of Galilean invariance breaking arises from the lattice itself.

We investigate the effect of Galilean invariance breaking and restore the Galilean invariance on the lattice by studying the dispersion relation and proton-neutron scattering phase shifts. We find that analyzing the phase shifts in different frames is useful to detect GIB for the $^1S_0$ partial wave while the dispersion relation provides a more efficient tool in the $^3S_1$ channel. This
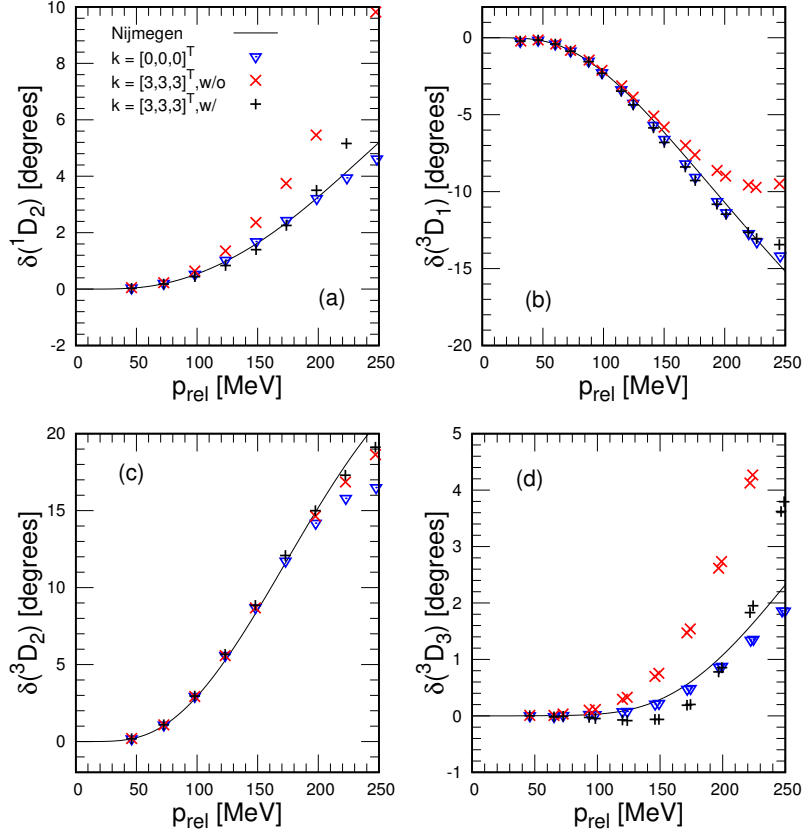
FIG. 7. (Color online) D-wave neutron-proton scattering phase as a function of the relative momenta between the proton and neutron. The spherical wall method is used.

is because the $^1S_0$ ground state is a continuum state while the ground state of $^3S_1$ is a bound state.

We find that the Galilean invariance breaking caused by the nonlocal smearing parameter s_{NL} partially cancels that caused by the lattice artifacts due to the nonzero lattice spacing. Due to this cancellation, the Galilean invariance breaking of the NN interaction at N3LO is small. After including the GIR correction the Galilean invariance is restored. One should notice that similar calculations would have to be repeated if altering any details such as the lattice spacing or other terms in the Hamiltonian.

Our previous study shows that the non-locally smeared contact operators are promising in generating the binding of nucleons in nuclei. The present study shows the Galilean invariance breaking is small, and the Galilean invariance can be restored after including the Galilean invariance restoration corrections. This interaction has been used in Monte Carlo simulations for the nuclear binding of the light- and medium-mass nuclei. We hope to be able to report the corresponding results in the near future.

Appendix A: Lattice operator definitions

The pertinent lattice operators were already defined in Ref. [13]. However, for completeness, we list them again here. With the dressed annihilation operator $a_{i,j}^{s_{\mathrm{NL}}}$, we define the pair annihilation operators $[a(\mathbf{n})a(\mathbf{n}')]_{S,S_z,I,I_z}^{s_{\mathrm{NL}}}$, where

$$[a(\mathbf{n})a(\mathbf{n}')]_{S,S_z,I,I_z}^{s_{\mathrm{NL}}} = \sum_{i,j,i',j'} a_{i,j}^{s_{\mathrm{NL}}}(\mathbf{n})M_{ii'}(S,S_z)M_{jj'}(I,I_z)a_{i',j'}^{s_{\mathrm{NL}}}(\mathbf{n}') \tag{A1}$$

with

$$M_{ii'}(0,0) = \frac{1}{\sqrt{2}}[\delta_{i,0}\delta_{i',1} - \delta_{i,1}\delta_{i',0}], \tag{A2}$$

$$M_{ii'}(1,1) = \delta_{i,0}\delta_{i',0}, \tag{A3}$$

$$M_{ii'}(1,0) = \frac{1}{\sqrt{2}}[\delta_{i,0}\delta_{i',1} + \delta_{i,1}\delta_{i',0}], \tag{A4}$$

$$M_{ii'}(1,-1) = \delta_{i,1}\delta_{i',1}. \tag{A5}$$

We define the lattice finite difference operation ∇_l on a general lattice function $f(\mathbf{n})$ as

$$\nabla_l f(\mathbf{n}) = \frac{1}{2}f(\mathbf{n}+\hat{\mathbf{l}}) - \frac{1}{2}f(\mathbf{n}-\hat{\mathbf{l}}), \tag{A6}$$

where $\hat{\mathbf{l}}$ is the spatial lattice unit vector in the l direction. It is also convenient to define the lattice finite difference operation $\nabla_{1/2,l}$ defined on points halfway between lattice sites,

$$\nabla_{1/2,l} f(\mathbf{n}) = f(\mathbf{n}+\frac{1}{2}\hat{\mathbf{l}}) - f(\mathbf{n}-\frac{1}{2}\hat{\mathbf{l}}). \tag{A7}$$

This operation is used solely to define the Laplace operator,

$$\nabla_{1/2}^2 = \sum_l \nabla_{1/2,l}^2 \, . \tag{A8}$$

Further, we define the solid harmonics

$$R_{L,L_z}(\mathbf{r}) = \sqrt{\frac{4\pi}{2L+1}}r^L Y_{L,L_z}(\theta,\phi), \tag{A9}$$

and their complex conjugates

$$R_{L,L_z}^*(\mathbf{r}) = \sqrt{\frac{4\pi}{2L+1}}r^L Y_{L,L_z}^*(\theta,\phi). \tag{A10}$$

Using the pair annihilation operators, lattice finite differences, and the solid harmonics, we define the operator

$$P_{S,S_z,L,L_z,I,I_z}^{2M,s_{\mathrm{NL}}}(\mathbf{n}) = [a(\mathbf{n})\nabla_{1/2}^{2M}R_{L,L_z}^*(\nabla)a(\mathbf{n})]_{S,S_z,I,I_z}^{s_{\mathrm{NL}}}, \tag{A11}$$

where $\nabla_{1/2}^{2M}$ and ∇ act on the second annihilation operator. More explicitly stated, this means that we act on the $\mathbf{n}'$ in Eq. (A1) and then set $\mathbf{n}'$ to equal $\mathbf{n}$. The even integer $2M$ gives us higher powers of the finite differences. Writing the Clebsch-Gordan coefficients as $\langle SS_z LL_z|JJ_z\rangle$, we define

$$O_{S,L,J,J_z,I,I_z}^{2M,s_{NL}}(\mathbf{n}) = \sum_{S_z,L_z} \langle SS_z LL_z|JJ_z\rangle P_{S,S_z,L,L_z,I,I_z}^{2M,s_{NL}}(\mathbf{n}). \tag{A12}$$

[1] S. Weinberg, Nucl. Phys. **B363**, 3 (1991).

[2] E. Epelbaum, W. Glöckle, and U.-G. Meißner, Nucl. Phys. **A637**, 107 (1998), arXiv:nucl-th/9801064 [nucl-th].

[3] E. Epelbaum, W. Glöckle, and U.-G. Meißner, Nucl. Phys. **A671**, 295 (2000), arXiv:nucl-th/9910064 [nucl-th].

[4] E. Epelbaum, W. Glöckle, and U.-G. Meißner, Nucl. Phys. **A747**, 362 (2005), arXiv:nucl-th/0405048 [nucl-th].

[5] E. Epelbaum, H.-W. Hammer, and U.-G. Meißner, Rev. Mod. Phys. **81**, 1773 (2009), arXiv:0811.1338 [nucl-th].

[6] R. Machleidt and D. R. Entem, Phys. Rept. **503**, 1 (2011), arXiv:1105.2919 [nucl-th].

[7] E. Epelbaum, H. Krebs, D. Lee, and U.-G. Meißner, Phys. Rev. Lett. **106**, 192501 (2011), arXiv:1101.2547 [nucl-th].

[8] E. Epelbaum, H. Krebs, T. A. Lähde, D. Lee, and U.-G. Meißner, Phys. Rev. Lett. **109**, 252501 (2012), arXiv:1208.1328 [nucl-th].

[9] E. Epelbaum, H. Krebs, T. A. Lähde, D. Lee, U.-G. Meißner, and G. Rupak, Phys. Rev. Lett. **112**, 102501 (2014), arXiv:1312.7703 [nucl-th].

[10] S. Elhatisari, D. Lee, G. Rupak, E. Epelbaum, H. Krebs, T. A. Lähde, T. Luu, and U.-G. Meißner, Nature **528**, 111 (2015), arXiv:1506.03513 [nucl-th].

[11] D. Lee, Prog. Part. Nucl. Phys. **63**, 117 (2009), arXiv:0804.3501 [nucl-th].

[12] S. Elhatisari *et al.*, Phys. Rev. Lett. **117**, 132501 (2016), arXiv:1602.04539 [nucl-th].

[13] N. Li, S. Elhatisari, E. Epelbaum, D. Lee, B.-N. Lu, and U.-G. Meißner, Phys. Rev. **C98**, 044002 (2018), arXiv:1806.07994 [nucl-th].

[14] D. Lee and R. Thomson, Phys. Rev. **C75**, 064003 (2007), arXiv:nucl-th/0701048 [nucl-th].

[15] B.-N. Lu, N. Li, S. Elhatisari, D. Lee, E. Epelbaum, and U.-G. Meißner, (2018), arXiv:1812.10928 [nucl-th].

[16] P. Reinert, H. Krebs, and E. Epelbaum, Eur. Phys. J. **A54**, 86 (2018), arXiv:1711.08821 [nucl-th].

[17] E. Epelbaum, H. Krebs, and U.-G. Meißner, Eur. Phys. J. **A51**, 53 (2015), arXiv:1412.0142 [nucl-th].

[18] N. Kaiser, Phys. Rev. **C64**, 057001 (2001), arXiv:nucl-th/0107064 [nucl-th].

[19] D. R. Entem, N. Kaiser, R. Machleidt, and Y. Nosyk, Phys. Rev. **C91**, 014002 (2015), arXiv:1411.5335 [nucl-th].

[20] M. Lüscher, Nucl. Phys. **B354**, 531 (1991).

[21] K. Rummukainen and S. A. Gottlieb, Nucl. Phys. **B450**, 397 (1995), arXiv:hep-lat/9503028 [hep-lat].

[22] C. h. Kim, C. T. Sachrajda, and S. R. Sharpe, Nucl. Phys. **B727**, 218 (2005), arXiv:hep-lat/0507006 [hep-lat].

[23] S. R. Beane, P. F. Bedaque, A. Parreno, and M. J. Savage, Phys. Lett. **B585**, 106 (2004), arXiv:hep-lat/0312004 [hep-lat].

[24] X. Feng, X. Li, and C. Liu, Phys. Rev. **D70**, 014505 (2004), arXiv:hep-lat/0404001 [hep-lat].

[25] M. Gockeler, R. Horsley, M. Lage, U.-G. Meißner, P. E. L. Rakow, A. Rusetsky, G. Schierholz, and J. M. Zanotti, Phys. Rev. **D86**, 094513 (2012), arXiv:1206.4141 [hep-lat].

[26] R. A. Briceno and Z. Davoudi, Phys. Rev. **D88**, 094507 (2013), arXiv:1204.1110 [hep-lat].

[27] R. A. Briceo, Z. Davoudi, T. Luu, and M. J. Savage, Phys. Rev. **D88**, 114507 (2013), arXiv:1309.3556 [hep-lat].

[28] R. A. Briceno, Z. Davoudi, and T. C. Luu, Phys. Rev. **D88**, 034502 (2013), arXiv:1305.4903 [hep-lat].

[29] B.-N. Lu, T. A. Lähde, D. Lee, and U.-G. Meißner, Phys. Lett. **B760**, 309 (2016), arXiv:1506.05652 [nucl-th].

[30] S. Elhatisari, D. Lee, U.-G. Meißner, and G. Rupak, Eur. Phys. J. **A52**, 174 (2016), arXiv:1603.02333 [nucl-th].

[31] H. P. Stapp, T. J. Ypsilantis, and N. Metropolis, Phys. Rev. **105**, 302 (1957).

[32] V. Baru, C. Hanhart, M. Hoferichter, B. Kubis, A. Nogga, and D. R. Phillips, Nucl. Phys. **A872**, 69 (2011), arXiv:1107.5509 [nucl-th].

[33] M. Hoferichter, J. Ruiz de Elvira, B. Kubis, and U.-G. Meißner, Phys. Rev. Lett. **115**, 192301 (2015), arXiv:1507.07552 [nucl-th].

[34] M. Döring, U. G. Meißner, E. Oset, and A. Rusetsky, Eur. Phys. J. **A48**, 114 (2012), arXiv:1205.4838 [hep-lat].